Journal of Nuclear Medicine, published on October 27, 2016 as doi:10.2967/jnumed.116.181768

(1) Preclinical Evaluation of ^{18}F-PSMA-1007: A New PSMA-Ligand for Prostate Cancer Imaging

(2) ^{18}F-PSMA-1007

(3) Jens Cardinale[1], Martin Schäfer[1], Martina Benešová[1], Ulrike Bauder-Wüst[1], Karin Leotta[2], Matthias Eder[1], Oliver C. Neels[1], Uwe Haberkorn[2], Frederik L. Giesel[2], Klaus Kopka[1]

(4) [1] German Cancer Research Center, Division of Radiopharmaceutical Chemistry, INF 280, 69120 Heidelberg; [2] University Hospital Heidelberg, Department of Nuclear Medicine, INF 400, 69120 Heidelberg

(5) Nothing

(6) Jens Cardinale, DKFZ, INF 280, 69120 Heidelberg, Tel.: +49 6221 42 2458, Fax: +49 6221 42 2434, email: j.cardinale[at]dkfz.de

(7) Jens Cardinale, DKFZ, INF 280, 69120 Heidelberg, Tel.: +49 6221 42 2458, Fax: +49 6221 42 2434, email: j.cardinale[at]dkfz.de

(8) **Word Count: 4913**

ABSTRACT

Introduction In recent years several radiotracers targeting the prostate-specific membrane antigen (PSMA) have been introduced. Few of those had a high clinical impact for the treatment of patients suffering from prostate cancer. However, the number of fluorine-18 labeled tracers addressing PSMA is still limited. Therefore, we aimed at the development of a radiofluorinated molecule with emphasis on resembling the structure of the therapeutic PSMA-617. **Methods** The non-radioactive reference compound PSMA-1007 and the labeling precursor were built up by solid phase chemistry. The radioligand ^{18}F-PSMA-1007 was produced via a two-step procedure using the prosthetic group 6-^{18}F-fluoronicotinic acid 2,3,5,6-tetrafluorophenyl ester (6-^{18}F-F-Py-TFP). The binding affinity of the ligand towards PSMA and its internalization properties were evaluated *in vitro* using PSMA-positive LNCaP (Lymph Node Carcinoma of the Prostate) cells. Further, organ distribution studies were performed using LNCaP- and PC-3 (Prostate Cancer cell line; PSMA negative) tumor bearing mice. Finally, a microPET (small animal Positron Emission Tomography) imaging with an LNCaP tumor bearing mouse was carried out. **Results** The identified ligand revealed a binding affinity of 6.7±1.7 nM towards PSMA and an exceptional high internalization ratio of 67±13 % *in vitro*. In organ distribution studies a high and specific tumor uptake of 8.0±2.4 %ID/g in LNCaP tumor bearing mice was observed. In further microPET experiments LNCaP tumors were clearly visualized. **Conclusion** The radiofluorinated PSMA-ligand showed promising characteristics in its preclinical evaluation and the feasibility of prostate cancer imaging was demonstrated by microPET studies. Thus, we recommend the ligand ^{18}F-PSMA-1007 for clinical transfer as diagnostic PET tracer for prestaging and monitoring of prostate cancer.

Key Words PSMA, Fluorine-18, Prostate Cancer, PET

INTRODUCTION

The prostate-specific membrane antigen (PSMA) is strongly overexpressed in most prostate cancers, and offers a versatile target for imaging and therapy (*1*). Therefore, a number of PSMA-targeting tracers have been developed over the past two decades (*2*). Some of the clinically most potent compounds are listed in Table 1.

Two major contributions to the field are represented by the urea based peptidomimetic substances PSMA-11 (*3*) and PSMA-617 (*4*) (Fig. 1). While both compounds can be labeled with the short living radioisotope Ga-68, the latter offers broader opportunities for labeling via the DOTA chelator including ^{177}Lu and ^{225}Ac.

Gallium-68 labeled PSMA-11 was introduced in 2012 (*3*) and, after its clinical application (*5*), quickly evolved to the most commonly used radiotracer for PSMA-PET imaging of prostate cancer (*1*). The radionuclide ^{68}Ga is introduced to PSMA-11 via the chelator N,N´-*bis*[2-hydroxy-5-(ethylene-β-carboxy)benzyl]ethylenediamine-N,N´-diacetic acid (HBED-CC). However, the chelating agent HBED-CC cannot form stable complexes with the trivalent therapeutic radionuclides ^{177}Lu, ^{90}Y, and ^{225}Ac. Hence, a compound bearing a DOTA-chelator while maintaining the binding properties of PSMA-11 was of high clinical interest. As a consequence, PSMA-617 was designed and introduced in 2015 (*4*). The structural key element of PSMA-617 is its linker design, which triggers binding and internalization of the substance by a presumed interaction of the lipophilic (tranexamic acid) and aromatic (2-naphthylalanine) amino acids with lipophilic parts of the PSMA binding pocket (*6*). Although prospective clinical trials are still pending, the ^{177}Lu and ^{225}Ac labeled version of this PSMA inhibitor already proved its therapeutic potential (*7*-*14*).

Principally both – ^{68}Ga-PSMA-11 and PSMA-617 (^{177}Lu or ^{225}Ac labeled) – complete a good team covering the diagnostic and therapeutic aspects of clinical prostate cancer care. However, regarding Ga-

68 there is one major drawback related to the availability of the radionuclide: currently commercially available Ge-68/Ga-68 generators can offer a maximum activity of 1.85 GBq Ga-68 (88.9 % β^+, 67.71 min $t_{1/2}$), limiting the average batch production of the desired tracer to approximately 2 to 4 patient doses, depending on the usage of the radionuclide generator. An alternative is the cyclotron production of ^{68}Ga using a liquid target (*15*) but this method has so far not been established as standard for large scale production and thus cannot guarantee a reliable provision of the tracer. Together with the short half-life of ^{68}Ga this results in the necessity of several productions per day for sustaining the clinical routine. Hence, there is a strong demand for ^{18}F-labeled PSMA-targeting radiotracers (96.7 % β^+, 109.77 min $t_{1/2}$). In principle, such a compound is already available in form of 2-(3-(1-carboxy-5-[(6-[^{18}F]fluoro-pyridine-3-carbonyl)-amino]-pentyl)-ureido)-pentanedioic acid (also known as ^{18}F-DCFPyL) (*16*). However, we aimed towards a radiofluorinated tracer mimicking the biodistribution behavior of labeled PSMA-617, thereby making use of its adjusted linker design. Owing to the need of alternative ^{18}F-labeled PSMA tracers and to complete a theranostic tandem with ^{177}Lu-PSMA-617 we herein report the preclinical characterization of our leading candidate ^{18}F-PSMA-1007, which we recommended for first-in-man studies in patients suffering from prostate cancer (*17*).

MATERIALS AND METHODS

All chemicals, reagents and solvents used were at least synthesis grade, purchased from Sigma Aldrich, VWR, Iris Biotech and Carl Roth and used without further purification.

Where mean values are given the respective error was determined by standard deviation. In case of the *in vitro* experiments, each result from a single experiment was determined as triplicate or quadruplicate within the experiment, while the experiments were repeated multiple times. The error of

the mean values was then calculated by standard deviation ignoring the errors for the single experiment results.

The patient scan shown in figure 5 was taken from a first-in-man study which was ethically approved by the IRB of the University Hospital Heidelberg in accordance to the national regulations of Germany and the updated version of the Helsinki declaration (permit S321/2012).

Syntheses of the Precursor Molecules and the Reference Compound

The synthesis of *N*,*N*,*N*-trimethyl-5-((2,3,5,6-tetrafluorophenoxy)-carbonyl)pyridine-2-aminium trifluoromethansulfonate as precursor for the radiosynthesis of the prosthetic group 6-^{18}F-F-Py-TFPwas accomplished as described by Olberg et al. (*18*).

The syntheses of the precursor for ^{18}F-PSMA-1007 (compound 1) as well as the reference compound PSMA-1007 (compound 2) have been accomplished by well-established methods and are summarized in Fig. 2. Briefly, the binding motif consisting of the amino acids glutamine and lysine, linked via their α-amino groups by a carbonyl forming a urea group, was built up on solid phase from resin bound allyloxycarbonyl protected lysine 3 and the isocyanate of *bis*-*tert*-Butyl protected glutamic acid 4 (*3*). Subsequently the linker was built up by standard fluorenylmethoxycarbonyl (Fmoc) solid phase synthesis (*3*,*4*,*6*). Then, the labeling precursor 1 was prepared by cleavage from the resin and deprotection, while the non-radioactive reference compound 2 was prepared via the intermediate 7 and subsequent cleavage and deprotection.

Radiosynthesis of ^{18}F-PSMA-1007

Preparation and activation of the no carrier added ^{18}F-fluoride. Fluorine-18 was produced by irradiation of ^{18}O-enriched water (Rotem Industries Ltd.) with 16.5 MeV proton beams using the ^{18}O(p,n)^{18}F nuclear

reaction. Irradiations were performed with the Scanditronix MC32NI cyclotron at the Division of Radiopharmaceutical Chemistry of the German Cancer Research Center (dkfz) Heidelberg, Germany.

After transfer of the irradiated water to an automated radiosynthesizer system (Trasis AllInOne) $^{18}F\text{-}F^-$ was separated from irradiated $[^{18}O]H_2O$ by passing through a pre-conditioned (5 ml 1 M K_2CO_3 and 10 ml water) anion exchange cartridge (Waters Accel^{TM} Plus QMA Cartridge light) and subsequently eluted with a mixture of 800 µl acetonitrile and 150 µl tetrabutylammonium bicarbonate solution (320 mM in ultrapure water). The mixture was then evaporated to dryness at a temperature of 100 °C under a stream of nitrogen. This azeotropic drying was subsequently repeated two times by adding 1.8 ml of acetonitrile for each step. After applying maximum achievable vacuum to the reaction vessel for 90 seconds at 80 °C and subsequent cooling to 50 °C the dry residue was dissolved in 2 ml of *tert*-butanol/acetonitrile (8:2 v/v) and used for the radiolabeling reactions.

Preparation of no carrier added 6-^{18}F-F-Py-TFP. The preparation of the prosthetic group 6-^{18}F-F-Py-TFP was accomplished with a slight modification of the reported (*18*) procedure. After trapping of 6-^{18}F-F-Py-TFP on an Oasis MCX Plus Sep-Pak cartridge and subsequent washing steps, the cartridge was rinsed with the eluent (acetonitrile/water 65:35 v/v) in two fractions of 400 µl and 500 µl, respectively. While a negligible amount of radioactivity was contained in the first fraction, usually more than 50 % of the product activity was contained in the second fraction (typically 1.0 – 2.0 GBq), which was then used for the subsequent radiolabeling reactions.

^{18}F-PSMA-1007. 400 µl of 6-^{18}F-F-Py-TFP solution were mixed with 100 µl solution of 1 (2 mg/ml in DMSO; 220 nmol) in the presence of 100 µl phosphate buffer (0.2 molar, pH 9.0) and heated at 60 °C for 20 min. The product was separated from the crude mixture by semi-preparative high performance liquid chromatography (HPLC) (Column: Merck Chromolith® RP-18e 100-10 mm; multi step gradient: solvent A: Acetonitrile, solvent B: Water + 0.1 % TFA, 100 % B → 65 % B (2 min) →50 % B (6 min) → 5 % B (8 min) →

5 % B (10 min) with 4 ml / min flowrate; t_r = 4.37 min, product collected from 4.3 to 4.6 min). Subsequently, the product was concentrated on a SepPak C-18 cartridge (Waters) and finally eluted in 1 ml ethanol/water (70:30 v/v).

Formulation. For the formulation the amount of carrier was adjusted appropriately to the respective assays with radiometal labeled PSMA-ligands (where the "carrier" is the non-separated precursor peptide). Therefore the ethanol/water mixture containing ^{18}F-PSMA-1007 was dried at 98 °C under a stream of nitrogen and the product subsequently dissolved either in a 6 µmolar solution of non-radioactive reference 2 in 0.9 % NaCl for *in vitro* experiments (approx. 100 MBq/ml) or in a 0.6 µmolar solution of 2 in 0.9 % NaCl for organ distribution studies (approx. 10-20 MBq/ml). For the microPET experiment the product was dissolved in 0.9 % NaCl, the specific activity determined by HPLC, and the solution diluted to a final concentration of 0.6 µmol/l.

***In Vitro* Experiments**

Cell Culture. For binding studies and *in vivo* experiments LNCaP cells (metastatic lesion of human prostatic adenocarcinoma, ATCC® CRL-1740™) were cultured in RPMI 1640 (PAN Biotech) medium supplemented with 10% fetal calf serum and stable glutamine (PAN Biotech). Cells were grown at 37 °C in an incubator with humidified air, equilibrated with 5 % CO_2.

Cell Binding and Internalization. The competitive cell binding assays and internalization experiments were performed as described previously (*6*). Briefly, LNCaP cells (10^5 per well) were incubated with the ^{68}Ga-labeled radioligand [Glu-urea-Lys(Ahx)]$_2$-[^{68}Ga(HBED-CC)] (^{68}Ga-PSMA-10) (*19*) at a concentration of 0.75 nM in the presence of 12 different concentrations of 2 (0–5000 nM, 100 µL/well). After incubation, washing was carried out using a multiscreen vacuum manifold (Millipore, Billerica, MA). Cell-bound radioactivity was measured using a gamma counter (Packard Cobra II, GMI, Minnesota, USA). The 50 %

inhibitory concentrations (IC_{50}) were calculated by fitting the data using a nonlinear regression algorithm (GraphPad Prism 5.01 Software). Experiments were performed as quadruplicate.

To determine the specific cell uptake and internalization, 10^5 cells were seeded in poly-L-lysine coated 24-well cell culture plates for 24 h. The cells in each well were incubated with 250 µl of a 30 nM solution of c.a. ^{18}F-PSMA-1007 (15-20 GBq/µmol) in Opti-MEM I medium (Gibco). Specific cellular uptake was determined by blocking with 2-(phosphonomethyl)pentanedioic acid (2-PMPA) (500 µM final concentration, Axxora, Loerrach, Germany). All experiments were conducted at 37 °C and 4 °C. The incubation was terminated after 45 min by washing 3 times with 1 mL of ice-cold phosphate buffered saline. The cells were subsequently incubated twice with 0.5 mL glycine-HCl (50 mM, pH = 2.8) for 5 min each to remove the surface-bound fraction, the supernatant was collected. After an additional washing step with 1ml ice-cold phosphate buffered saline, the cells were lysed using 0.5 mL NaOH (0.3 N), collected and measured in a gamma counter. The specific cellular uptake was calculated as percent of the initially added radioactivity bound to 10^5 cells %IA/10^5 cells by subtraction of the respective uptake under blocking conditions. All Experiments were conducted as triplicate.

Plasma Stability. For the determination of the plasma stability 400 µl human plasma AB (Sigma-Aldrich) were incubated with 40 µl of the 6 µmolar c.a. ^{18}F-PSMA-1007 formulation (100 MBq / ml) at 37 °C. After 1, 2 and 4 hours samples of 100 µl were removed from the mixture, the protein precipitated by addition of 100 µl acetonitrile, separated from the liquid by centrifugation at 13000 rpm (two times) and the liquid analyzed by high performance liquid chromatography.

***In Vivo* and Organ Distribution Experiments**

All animal experiments were conducted in compliance with the current laws of the Federal Republic of Germany. For *in vivo* and organ distribution experiments, 8 week old male BALB/c nu/nu mice were subcutaneously inoculated into the right trunk with 6 x 10^6 LNCaP cells in 50% Matrigel or 5 x 10^6 PC-3

cells in Opti-MEM I medium (Gibco), respectively. The organ distribution studies were carried out when the size of tumor was approximately 1 cm^3.

Organ Distribution. Organ distribution studies were carried out with mice bearing an LNCaP tumor with and without 2-PMPA-blockade and mice bearing a PC-3 tumor. Each experiment was conducted in triplicate. In case of the blockade experiment, the mice were administered 0.4 mM 2-PMPA (100 µl; 40 nmol) via tail vein injection 30 minutes before injection of the tracer. PSMA-1007 was administered as 0.6 µM solution (100 µl; 60 pmol), spiked with 1-2 MBq ^{18}F-PSMA-1007, via the tail vein injection. At 1 h p. i., the animals were sacrificed (CO_2 asphyxiation), organs of interest were dissected, blotted dry and weighed. The radioactivity was measured with a gamma counter (Packard Cobra II, GMI, Minnesota, USA) and calculated as % ID/g.

Dynamic PET Experiments. For the microPET study 100 µl 0.6 µM c.a. ^{18}F-PSMA-1007 (approx. 420 GBq/µmol; 60 pmol; 25 MBq) were injected via a lateral tail vein into a mouse bearing an LNCaP tumor xenograft. The anaesthetized animal (2% sevoflurane, Abbott, Wiesbaden, Germany) was placed in prone position into the Inveon small animal PET scanner (Siemens, Knoxville, Tenn., USA) to perform a dynamic microPET scan. Prior to the scan the transmission was measured for 900 s using a rotating Co-57 source. Acquisition was started 3 s before the tracer was injected and continued for 3600 s in list mode. The radial field of view was 7.5 cm. A second scan was performed 2 h p.i.. Between the first and the second scan the mouse was allowed to wake up.

The scans were reconstructed using the software Acquisition Workplace (Siemens) with a 28 frame protocol (2 times 15 s, 8 times 30 s, 5 times 60 s, 5 times 120 s, 8 times 300s). The volumes of interest for the generation of the time-activity-curves were drawn manually over the respective organs. Reconstruction of the images was done with the OSEM 3D MAP algorithm (MAP iterations: 18, output interval: 20; Image x-y size 256, image z size 161; size of voxel: x,y: 0.43 mm, z: 0.796 mm).

RESULTS

Syntheses of Labeling Precursors molecules and Reference Compound

The results of the syntheses of the labeling precursor and the reference compound are summarized in Table 2. A production batch usually resulted in 20-50 mg of the desired product equivalent to a yield of 13-30 %.

Radiosynthesis of ^{18}F-PSMA-1007

The initial labeling reaction delivered the prosthetic group 6-^{18}F-F-Py-TFP in non-decay corrected yields of 30-60 % after a synthesis time of 10 to 15 minutes (including cartridge separation). The final coupling delivered the labeled product ^{18}F-PSMA-1007 in yields of 5-10 % after an additional synthesis time of 30 minutes (including HPLC separation). Thus, the non-decay corrected yield was 1.5-6.0 % overall (typically 40-160 MBq in 600 µl reaction solvent) after approx. 45 minutes total synthesis time (without drying of the fluoride and formulation steps).

In Vitro Experiments

Competitive cell binding experiments on LNCaP cells against PSMA-10 revealed a nanomolar inhibition potency towards PSMA (K_i = 6.7±1.7 nM; n = 3). Moreover, the surface bound and internalized fraction of ^{18}F-PSMA-1007 on LNCaP cells was determined (n = 10) with 2.14±0.64 %IA/10^5 cells and 5.01±2.70 %IA/10^5 cells, respectively, leading to a total internalization ratio of 67±13 % (internalized / total bound activity). The respective values for PSMA-617 determined by the same procedures are a K_i of 2.3±2.9 nM with 1.1±0.7 %IA/10^5 cells surface bound and 1.6±0.4 %IA/10^5 cells internalized (both values calculated from the respective values bound per 10^6 cells by division with 10), leading to a total internalization ratio of 58 % (*6*). In the plasma stability test we did not observe any decomposition after 4 h (radiochemical purity > 99%) by high performance liquid chromatography.

In Vivo and Organ Distribution Experiments

The results of the organ distribution experiments are summarized in Table 3 and the results of the microPET experiment are shown in Figures 3 and 4. The SUV_{mean} BW values between 120 and 140 minutes p.i. were 0.23 (heart), 0.20 (liver), 7.6 (kidneys), 27.2 (bladder), 0.13 (muscle), 0.16 (bone) and 1.6 (tumor) resulting in a tumor-to-muscle ratio of 12.3 and a tumor-to-blood ratio of 7.0.

The time-activity curves (Fig. 3) show a fast uptake in the tumor and rapid clearance from non-target organs except for the kidneys. The tracer shows some uptake in the bone which declines over the time so that defluorination of the tracer can be excluded. Directly after administration the tumor-to-muscle and tumor-to-blood ratios start to increase constantly over time (Fig. 3). This result is also reflected in the maximum intensity projections shown in Fig. 4. The tumor becomes visible between 20 and 40 min p.i. showing a constantly improving contrast over the following hour.

DISCUSSION

The main goal of our study was the identification of an ^{18}F-labeled PSMA ligand based on the structure of PSMA-617 to complete a theranostic tandem with ^{177}Lu-PSMA-617. Within an extensive preclinical study, which will be reported elsewhere, ^{18}F-PSMA-1007 was identified as leading candidate for that purpose. Hence, we report here the preclinical characterization of ^{18}F-PSMA-1007.

Syntheses of Labeling Precursors molecules and Reference Compound

The preparation of the labeling precursor 1 and non-radioactive reference compound 2 (PSMA-1007) could easily be accomplished in analogy to previously described methods delivering sufficient amounts of material for preclinical investigations in adequate purity.

Radiosynthesis of ^{18}F-PSMA-1007

The preparation of the secondary labeling precursor 6-^{18}F-F-Py-TFP was reproducible and proved to be convenient due its separation by cartridge extraction. However, the conjugation of this prosthetic group to the peptidomimetic precursor 1 delivered the desired product ^{18}F-PSMA-1007 only in low yields of 5 to 10 %. This can be explained by a presumed inner salt formation in the terminal glutamic acid, which can lead to a reduced reactivity of the amino group towards the 2,3,5,6-tetrafluorophenyl ester. Only low amounts of radioactivity were required for the preclinical experiments and the purity of the product was sufficient.

***In Vitro* Experiments**

The urea-based peptidomimetic compound 2 shows a nanomolar binding affinity towards PSMA. Moreover, we could confirm a high and specific uptake of ^{18}F-PSMA-1007 in PSMA-positive LNCaP cells. This result was expected due to the high similarity of the compound 2 with the lead structure, which in turn was the leading candidate for imaging and therapy of prostate cancer selected from a library of PSMA-ligands (*6*). Surprisingly, a high internalization ratio of 67 % could be observed in our *in vitro* experiments (for comparison: the respective Value for PSMA-617 is 58 %) (*6*).

***In Vivo* and Organ Distribution Experiments**

In following organ distribution experiments the radiotracer revealed a high tumor uptake of 8.0±2.4 %ID/g 1h after administration. The uptake in non-target tissue was rather low, except for spleen and kidneys. However, this was expected at least for the kidneys since PSMA is also expressed there (*20*). This is also reflected in the results from the blockade experiments (vide infra) as a significant reduction of the uptake in both organs was observed indicating that the uptake in spleen is also specific.

Further organ distribution experiments were conducted for proving the specificity of the tumor uptake. The here presented blockade experiment using 2-PMPA as competing ligand led to a significant but not

complete, reduction of the tumor uptake. This might be attributed to the binding mechanism of 2-PMPA as it is reported to be a fast and reversible inhibitor (*21*). Considering the high internalization ratio of ^{18}F-PSMA-1007 only a small fraction of the ligand needs to be bound for being internalized even in the presence of the competitor and might thus result in a significant uptake into the tumor. A higher amount of blocking substance might further reduces the uptake of ^{18}F-PSMA-1007. An additional organ distribution experiment with PSMA negative PC-3 tumor-bearing mice showed a low tumor uptake of about 1.1±0.1 %ID/g. In summary, the uptake of ^{18}F-PSMA-1007 could be blocked by a sufficient amount of 2-PMPA, indicating a high specificity of the tracer.

Finally, the feasibility of prostate cancer imaging with ^{18}F-PSMA-1007 was demonstrated in a dynamic PET experiment with a mouse bearing an LNCaP tumor. The tracer shows the typical uptake in the kidneys and clearance via the renal pathway. However, the tumor was clearly visualized 40 minutes p.i. and the uptake in all non-target organs except for the kidneys declines over time leading to constantly improving tumor-to-background ratios. Thus, we clearly demonstrate the feasibility of PET imaging of prostate cancer using ^{18}F-PSMA-1007 as new radiotracer.

Outlook

Currently a first-in-man study is conducted with ^{18}F-PSMA-1007. Therefore a GMP-compliant (2-step) synthesis of the tracer has been developed, which will be published elsewhere. As an example one of the first PET-images acquired within this study is shown in Figure 5. Shown is a 76 year old patient with elevated PSA-level referred to the nuclear medicine to undergo a PSMA-PET/CT prior to surgery. The PSMA-PET detected an intraprostatic PSMA-Accumulation in the peripheral apical Zone on the right without any suspicious of tumor spread outside the prostate gland. This result clearly underlines the successful translation into a clinical setting.

CONCLUSION

Currently fluorine-18 labeled PSMA-targeting ligands are strongly needed for the clinical diagnosis of prostate cancer by means of PET/CT and PET/MRI. As part of an extended preclinical study the compound ^{18}F-PSMA-1007 was identified as leading diagnostic candidate for non-invasive PET imaging of prostate cancer. ^{18}F-PSMA-1007 might also be useful for planning PSMA ligand therapy with its therapeutic counterpart PSMA-617. The ligand shows promising binding and internalization properties *in vitro* as well as a high and specific uptake *in vivo*. The feasibility of prostate cancer imaging with ^{18}F-PSMA-1007 has further been demonstrated by a dynamic microPET experiment.

ACKNOWLEDGMENTS

This project was supported with a postdoc scholarship by ABX Advanced Biochemical Compounds GmbH (DKFZ file no.: L-15309). We thank Yvonne Remde for the support in establishing the radiosynthesis of ^{18}F-PSMA-1007 and Oksana Hautzinger and Uschi Schierbaum for their support with the organ distribution and microPET experiments.

REFERENCES

1. Rowe SP, Gorin MA, Allaf ME, et al. PET imaging of prostate-specific membrane antigen in prostate cancer: current state of the art and future challanges. *Prostate Cancer Prostatic Dis*. 2016;19:223-230.

2. Kiess AP, Banerjee SR, Mease RC, et al. Prostate-specific membrane antigen as a target for cancer imaging and therapy. *Q J Nucl Med Mol Imaging*. 2015;59:241-268.

3. Eder M, Schäfer M, Bauder-Wüst U, et al. ^{68}Ga-Complex lipophilicity and the targeting property of a urea-based PSMA inhibitor for PET imaging. *Bioconjug Chem*. 2012;23:688-697.

4. Benešová M, Schäfer M, Bauder-Wüst U, et al. Preclinical evaluation of a tailor-made DOTA-conjugated PSMA inhibitor with optimized linker moiety for imaging and endoratiotherapy of prostate cancer. *J Nucl Med*. 2015;56:914-920.

5. Afshar-Oromieh A, Haberkorn U, Eder M, Eisenhut M, Zechmann CM. [^{68}Ga]Gallium-labelled PSMA ligand as superior PET tracer for the diagnosis of prostate cancer: comparison with ^{18}F-FECH. *Eur J Nucl Med Mol Imaging*. 2012;39:1085-1086.

6. Benešová M, Bauder-Wüst U, Schäfer M, et al. linker modification strategies to control the prostate-specific membrane antigen (PSMA)-targeting and pharmacokinetic properties of DOTA-conjugated PSMA iInhibitors. *J Med Chem*. 2015;59:1761-1775.

7. Kratochwil C, Giesel FL, Stefanova M, et al. PSMA-targeted radionuclide therapy of metastatic castration-resistant prostate cancer with Lu-177 labeled PSMA-617. *J Nucl Med*. 2016;57:1170-1176.

8. Delker A, Fendler WP, Kratochwil C, et al. Dosimetry for ^{177}Lu-DKFZ-PSMA-617: a new radiopharmaceutical for the treatment of metastatic prostate cancer. *Eur J Nucl Med Mol Imaging*. 2016;43:42-51.

9. Rahbar K, Schmidt M, Heinzel A, et al. Response and tolerability of single dose of ^{177}Lu-PSMA-DKFZ-617 in patients with metastatic castration-resistant prostate cancer: a multicenter retrospective analysis. *J Nucl Med*. 2016;57:1334-1338.

10. Das T, Guleria M, Parab A, et al. Clinical translation of ^{177}Lu-labeled PSMA-617: Initial experience in prostate cancer patients. *Nucl Med Biol*. 2016;43:296-302.

11. Kabasakal L, AbuQbeitah M, Aygün A, et al. Pre-therapeutic dosimetry of normal organs and tissues of ^{177}Lu-PSMA-617 prostate-specific membrane antigen (PSMA) inhibitor in patients with castration-resistant prostate cancer. *Eur J Nucl Med Mol Imaging*. 2015;42:1976-1983.

12. Schlenkhoff CD, Gaestner F, Essler M, Schmidt M, Ahmadzadehfar H. Positive influence of 177Lu PSMA-617 therapy on bone marrow depression caused by metastatic prostate cancer. *Clin Nucl Med*. 2016; 41:522-528.

13. Hohberg M, Eschner W, Schmidt M, et al. Lacrimal glands may represent organs at risk for radionuclide therapy of prostate cancer with [^{177}Lu]DKFZ-PSMA-617. *Mol Imaging and Biol*. 2016;18:437-445.

14. Kratochwil C, Bruchertseifer F, Giesel FL, et al. ^{225}Ac-PSMA-617 for PSMA targeting alpha-radiation therapy of patients with metastatic castration-resistant prostate cancer. *J Nucl Med*. 2016; Ahead of print; doi:10.2967/jnumed.116.178673.

15. Pandey MK, Byrne JF, Jiang H, Packard AB, DeGrado TR. Cyclotron production of ^{68}Ga via the ^{68}Zn(*p*,*n*)^{68}Ga reaction in aqueous solution. *Am J Nucl Med Mol Imaging*. 2014;4:303-310.

16. Chen Y, Pullambhatla M, Byun Y, et al. 2-(3-{1-Carboxy-5-[(6-[^{18}F]fluoro-pyridine-3-carbonyl)-amino]-pentyl}ereido)-pentanediodic acid, [^{18}F]DCFPyL, a PSMA-based PET imaging agent for prostate cancer. *Clin Cancer Res*. 2011;11:7645.

17. Giesel FL, Cardinale J, Schäfer M, et al. ^{18}F-Labelled PSMA-1007 shows similarity in structure, biodistribution and tumor uptake to the theragnostic compound PSMA-617. *Eur J Nucl Med Mol Imaging*. 2016;43:1229-1230.

18. Olberg DE, Arukwe JM, Grace D, et al. One step radiosynthesis of 6-[^{18}F]fluoronicotinic acid 2,3,5,6-tetraflourophenyl ester ([^{18}F]-F-Py-TFP): A new prosthetic group for the efficient labeling of biomolecules with fluorine-18. *J Med Chem*. 2010;53:1732-1740.

19. Schäfer M, Bauder-Wüst U, Leotta K, et al. A dimerized urea-based inhibitor of the prostate-specific membrane antigen for ^{68}Ga-PET imaging of prostate cancer. *EJNMMI Res*. 2012;2:23.

20. Bacich DJ, Pinto JT, Tong WP, Heston WDW. Cloning, expression, genomic localization, and enzymatic activities of the mouse homolog of prostate-specific membrane antigen/NAALADase/folat hydrolase. *Mamm Genome*. 2001;12:117-123.

21. Liu T, Toriyabe Y, Kazak M, Berkman CE. Pseudoirreversible inhibition of prostate-specific membrane antigen by phosphoramidate peptidomimetics. *Biochemistry*. 2008;47:12658-12660.

22. Barett JA, Coleman RE, Goldsmith SJ, et al. First-in-man evaluation of 2 high-affinity PSMA-avid small molecules for imaging prostate cancer. *J Nucl Med*. 2013;54:380-387.

23. Zechmann CM, Afshar-Oromieh A, Armor T, et al. Radiation dosimetry and first therapy results with a ^{124}I/^{131}I-labeled small molecule (MIP-1095) targeting PSMA for prostate cancer therapy. *Eur J Nucl Med Mol Imaging*. 2014;41:1280-1292.

24. Vallabhajosula S, Nikolopoulou A, Babich JW, et al. ^{99m}Tc-Labeled small-molecule inhibitors of prostate-specific membrane antigen: Pharmacokinetics and biodistribution studies in healthy subjects and patients with metastatic prostate cancer. *J Nucl Med*. 2014;55:1791-1798.

25. Cho SY, Gage KL, Mease RC, et al. Biodistribution, tumor detection, and radiation dosimetry of ^{18}F-DCFBC, a low-molecular-weight inhibitor of prostate-specific membrane antigen, in patients with metastatic prostate cancer. *J Nucl Med*. 2012;53:1883-1891.

26. Rowe SP, Macura KJ, Mena E, et al. PSMA-based [^{18}F]DCFPyL PET/CT is superior to conventional imaging for lesion detection in patients with metastatic prostate cancer. *Mol Imaging Biol*. 2016;18:411-419.

27. Weineisen M, Schottelius M, Simecek J, et al. ^{68}Ga- and ^{177}Lu-labeled PSMA I&T: Optimization of a PSMA-targeted theranostic concept and first proof-of-concept human studies. *J Nucl Med*. 2015;56:1169-1176.

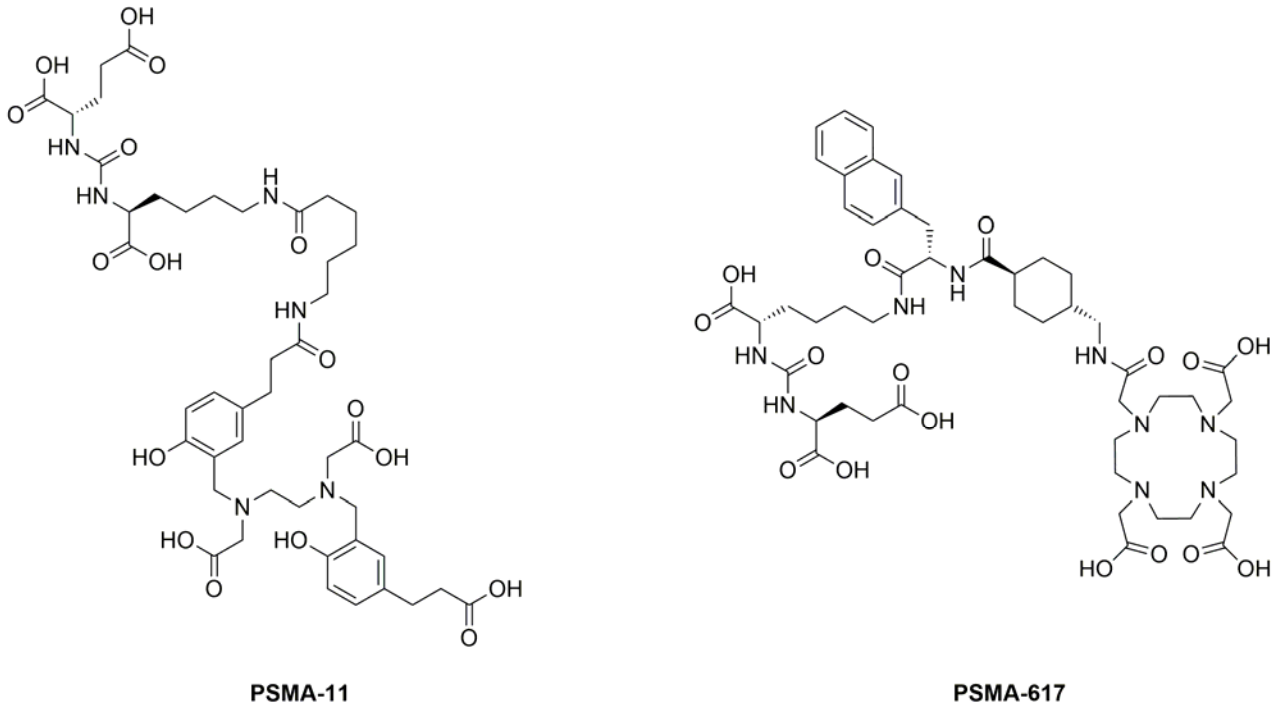

Figure 1: Chemical structures of PSMA-11 and PSMA-617 (lead structure)

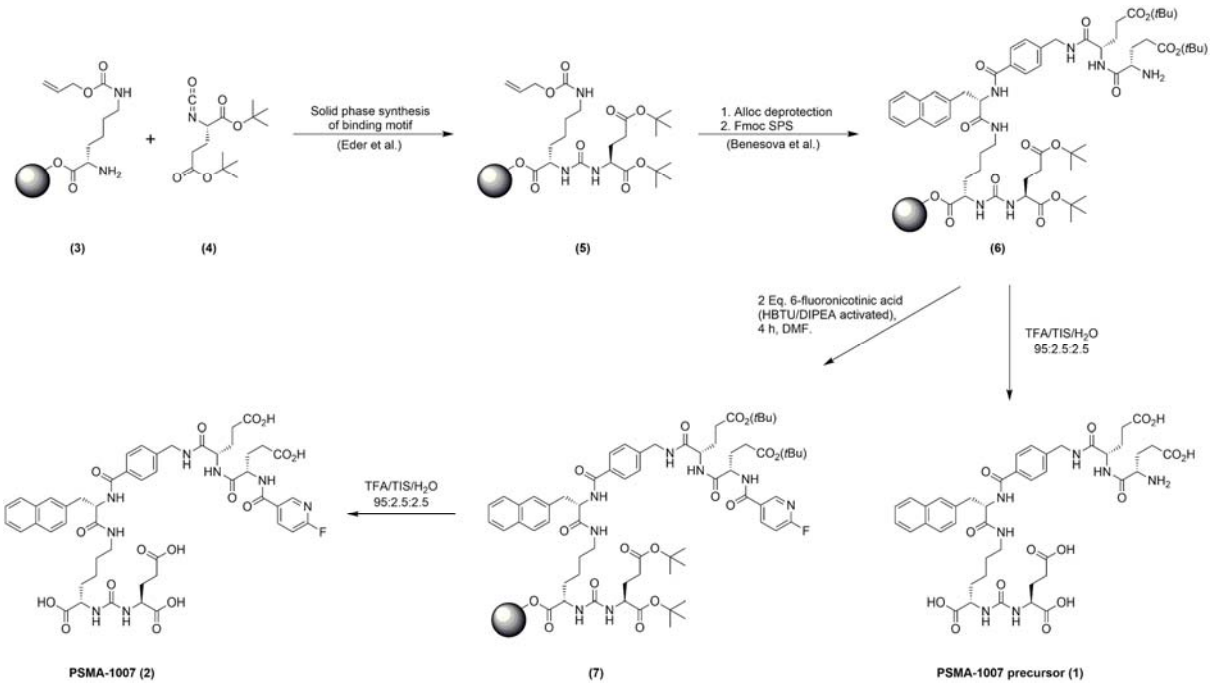

Figure 2 Synthesis of the labeling precursor (1) and PSMA-1007 (2)

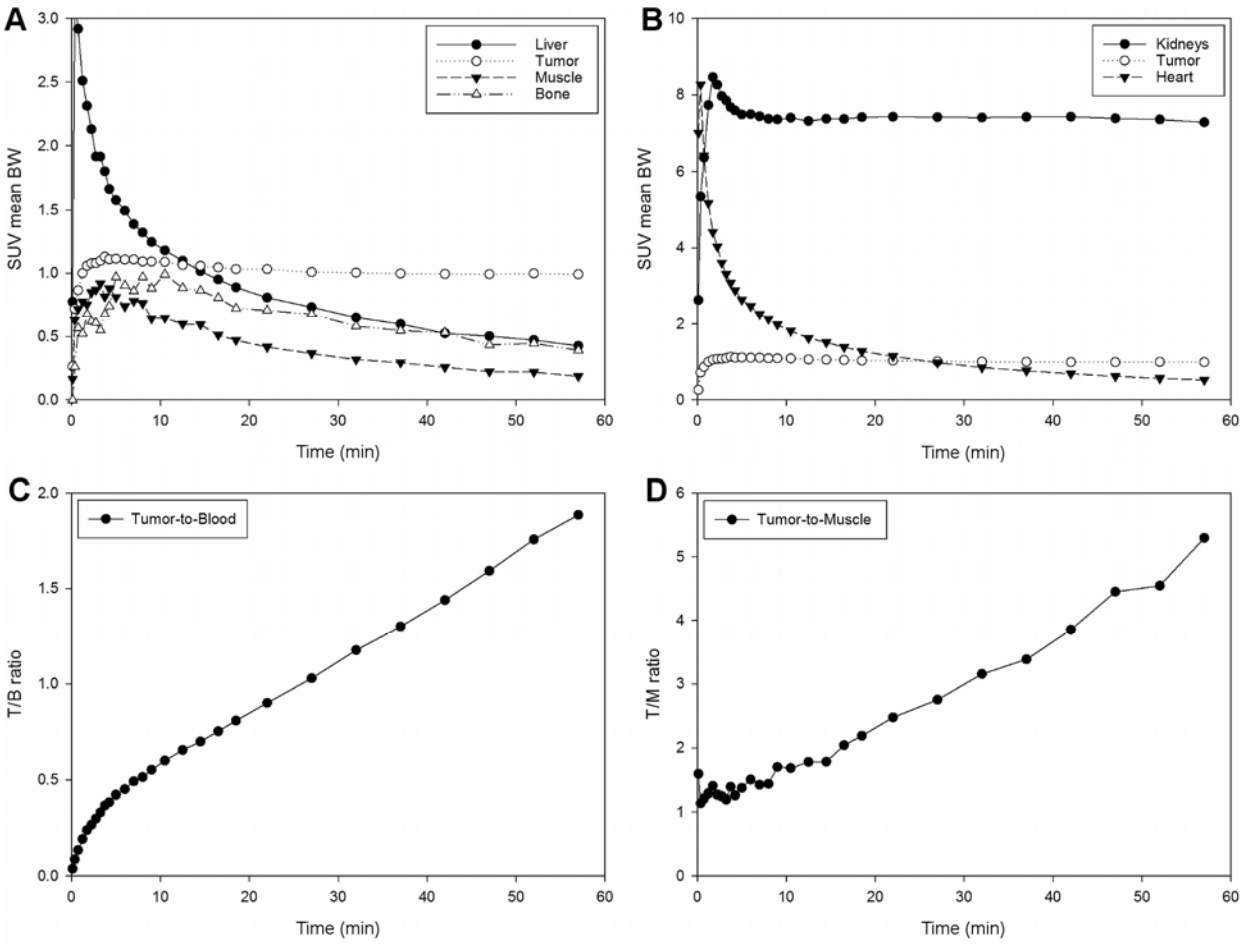

Figure 3: (A,B) Time-activity curves of the microPET experiment with a BALB/c nu/nu mouse bearing an LNCaP tumor after injection of 25 MBq c.a. ^{18}F-PSMA-1007 and corresponding (C) T/B (calculated from SUV mean Heart) and (D) T/M-ratios.

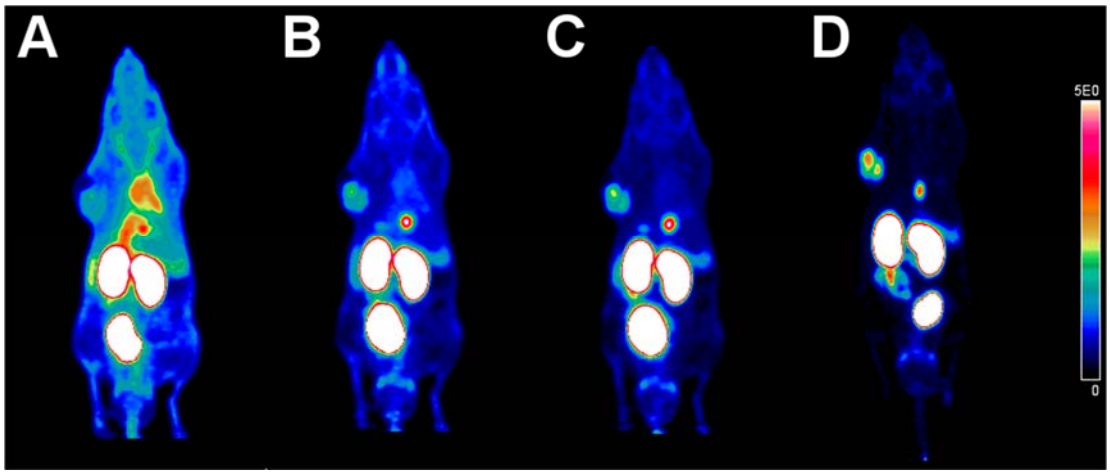

Figure 4: Whole-body coronal micro PET scans as maximum intensity projections of a BALB/c nu/nu mouse bearing a LNCaP tumor (A) 0-20, (B) 20-40, (C) 40-60, and (D) 120-140 min after injection of 25 MBq ^{18}F-PSMA-1007 (approx. 60 pmol).

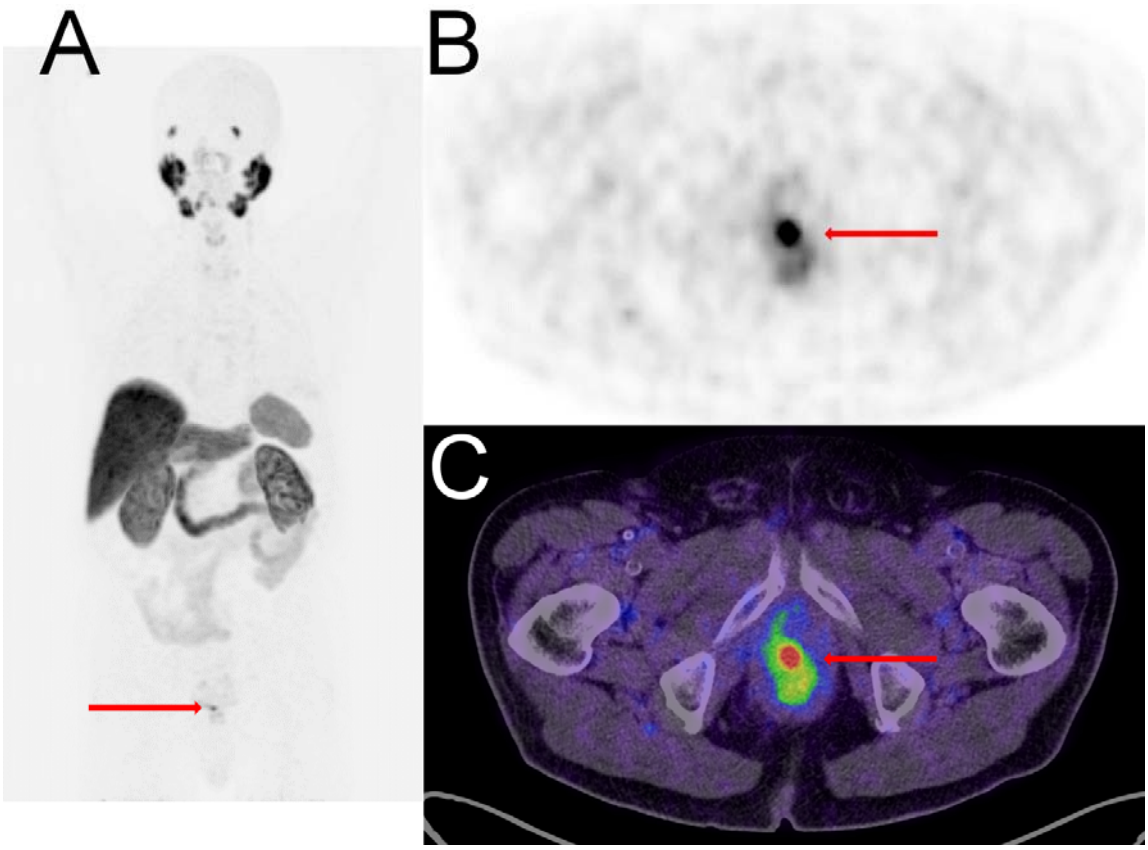

Figure 5: PET/CT of a patient suffering from prostate cancer 1 h after injection of ^{18}F-PSMA-1007. The red arrow is showing the lesion. (A) Maximum intensity projection. (B) Axial view of the pelvic region. (C) Fusion of PET-scan and CT (pelvic region; axial view)

Table 1: Some clinically relevant PSMA targeting molecules

Compound	Class	Label	Reference
MIP-1095	Therapeutic	^{124}I, ^{131}I	(*22*,*23*)
MIP-1404	Diagnostic	^{99m}Tc	(*24*)
DCFBC	Diagnostic	^{18}F	(*25*)
DCFPyL	Diagnostic	^{18}F	(*26*)
PSMA I&T	Theranostic	^{68}Ga, ^{177}Lu	(*27*)
PSMA-11	Diagnostic	^{68}Ga	(*3*)
PSMA-617	Theranostic	^{68}Ga, ^{90}Y, ^{177}Lu, ^{225}Ac	(*4*)

Table 2: Summary of the analytical results for compounds 1 and 2

Compound	m/z calc.	m/z found	t_{ret} HPLC	Purity (HPLC)
1	908,93	908.7	3.74 min	>97.3 % (254 nm) / >97,3 % (220 nm)
2	1032.01	1032.1	4.49 min	>96.5 % (254 nm) / >98.1 % (220 nm)

HPLC (Gradient: 5% A / 95 % B – 95 % A / 5 % B in 12.5 min; Flow: 3 ml / min; Column: Merck Chromolith® Performance RP-18e 100-4.6 mm; Solvent A: Acetonitrile, Solvent B: 0.1 % aqueous TFA; t_{dead}: 0.56 min (thiourea))

Table 3: Results of the organ distribution experiments at 1h p.i.: All mice were injected with 1-2 MBq ^{18}F-PSMA-1007 (c.a.; 60 pmol/injection). The mice were either bearing PSMA-positive LNCaP or PSMA-negative PC-3 tumors. In the blockade experiment the tracer was injected 30 minutes after administration of 40 nmol 2-PMPA (n = 3 mice per column).

	Uptake [%ID/g]		
Organ	LNCaP Tumor No blockade	LNCaP Tumor 2-PMPA blockade	PC-3 tumor (PSMA-negative)
Blood	0.60±0.21	0.41±0.13	0.77±0.29
Heart	1.11±0.20	0.41±0.07	1.45±0.10
Lung	1.25±0.27	0.78±0.04	2.09±0.33
Spleen	6.99±1.04	1.40±0.27	12.44±5.98
Liver	1.06±0.20	0.43±0.03	1.14±0.16
Kidney	84.03±13.85	9.72±2.50	142.08±25.82
Muscle	0.79±0.28	0.40±0.19	0.94±0.47
Small intestines	0.90±0.21	0.46±0.10	1.20±0.18
Brain	0.12±0.04	0.07±0.03	0.10±0.01
Tumor	8.04±2.39	4.26±2.06	1.05±0.11